

Carrier lifetime versus ion-implantation dose in silicon on sapphire

F. E. Doany, D. Grischkowsky, and C.-C. Chi

IBM T. J. Watson Research Center, P. O. Box 218, Yorktown Heights, New York 10598

(Received 10 November 1986; accepted for publication 16 December 1986)

We have measured the dependence of the free-carrier lifetime on O^+ ion-implantation dose in silicon-on-sapphire. At low implant doses, the carrier trapping rate increased linearly with the trap density introduced by ion implantation. At doses above $3 \times 10^{14} \text{ cm}^{-2}$ the measured carrier lifetime reached a limit of 600 fs.

The generation of short electrical pulses via optical methods has for some time been performed by driving Auston switches (photoconductive gaps) with short laser pulses.¹ The same techniques can also measure the generated electrical pulses by sampling methods. An alternate measurement approach has been to use the electro-optic effect in a nonlinear crystal.² In this case, the field of the electrical pulse is sampled through the rotation of the polarization of the optical sampling pulse. Because the electro-optic method has demonstrated 460 fs time resolution,³ it is presently considered to be the fastest measurement technique. However, in recent work photoconductive switches have generated and measured subpicosecond electrical pulses.⁴ This order of magnitude reduction in the generated pulsewidth demonstrates the ultrafast capability of the Auston switches and challenges the ultrafast time resolution of electro-optic methods. The shape of the electrical pulse generated by the Auston switch depends on the laser pulse shape, the nature of the charge source and the characteristics of the electrical transmission line, and the material properties of the semiconductor. Since laser pulses shorter than 100 fs are routinely obtained from colliding-pulse-mode-locked dye lasers, the laser pulse width can be made negligible compared to the generated electrical pulse. Furthermore, the limiting factors on the time response due to the circuit reactance may be eliminated if the capacitance of the generation site is reduced to negligible amounts. Under these conditions the duration of the electrical pulse would be mainly determined by the carrier lifetime in the semiconducting materials. However, until the measurements presented here, the limits of the carrier lifetimes obtainable were not known.

Although a variety of photoconductive materials has been used in picosecond optoelectronic devices,¹⁻⁵ ion-implanted silicon-on-sapphire (SOS) and amorphous silicon have proven to be the fastest materials due to their relatively short free-carrier lifetimes. The reduction of the free-carrier lifetimes is the result of the introduction of defects into the crystalline semiconductor which act as traps and recombination centers. With increasing doses of ion implantation, a systematic series of materials ranging from low defect density to amorphous can be produced thus facilitating studies of the dependence of carrier lifetimes on the density of traps. Previous studies on O^+ implantation dosage deduced carrier lifetimes from photoconductivity measurements and were limited to about 8 ps by laser pulse widths and circuit response times.⁶ Later work used a Hertzian dipole configuration of fast photoconductive switches fabricated from ion-

implanted SOS to generate and detect freely propagating 1.6 ps electrical pulses,⁷ thereby demonstrating that the carrier lifetime was at least this fast. The work describing the generation of subpicosecond electrical pulses⁴ ascribed the measured pulse limit to circuit parameters, and a numerical analysis was consistent with a carrier lifetime of 250 fs. In this work we present direct measurements of the carrier lifetimes of a systematic series of SOS samples with a wide range of defect densities introduced through ion implantation.

Optical excitation of silicon generates an electron-hole plasma. The temporal and spatial evolution of the photogenerated free carriers can be probed directly by time-resolved reflectivity and transmission measurements. The contribution of the $e-h$ plasma to the reflectivity (and transmission) can be estimated from the Drude expression for the refractive index:

$$n = n_0(1 - \omega_p^2/\omega^2)^{1/2}, \quad (1)$$

where n_0 is the refractive index of the silicon, ω is the probe angular frequency, and the plasma angular frequency ω_p is given by

$$\omega_p^2 = 4\pi N_e e^2/\epsilon m^*. \quad (2)$$

In the above expression N_e is the electron density, m^* is the reduced effective mass for electrons and holes, and ϵ is the background dielectric constant. At high excitation levels, the plasma frequency will exceed the probing frequency. In this case, the index of refraction becomes imaginary leading to strong reflection. At low excitation levels the plasma frequency is less than the probe frequency resulting in a decrease in reflectivity. For the low levels of excitation ($\omega_p < \omega$) the fractional index change due to the $e-h$ plasma is directly proportional to the carrier density:

$$\Delta n/n_0 = - (2\pi e^2/\epsilon m^* \omega^2) N_e. \quad (3)$$

Numerous experiments have been carried out to investigate the kinetics of laser-generated electron-hole plasmas and their influence on phase transitions in silicon.⁸⁻¹² These experiments used amplified picosecond and femtosecond optical pulses to investigate ultrafast heating dynamics in silicon following pulsed excitation near the melting threshold fluence of approximately 0.1 J cm^{-2} (carrier density $> 10^{20} \text{ cm}^{-3}$). At these excitation levels, the reflectivity dynamics are dominated by Auger recombination with carrier-density-dependent rates,^{11,12} plasma diffusion in bulk silicon,¹⁰ and lattice heating produced primarily by Auger recombination.^{9,11,12} In addition, these high pump laser fluences, even below the melting threshold, can produce temperature in-

creases of several $100\text{ }^\circ\text{C}$ ^{9,11} which can partially anneal out the lattice defects. In our experiment the pump laser fluence is kept approximately four to five orders of magnitude below the melting threshold in order to minimize lattice heating effects and carrier-carrier recombination processes (e.g. Auger recombination). The low carrier densities used here (10^{16} – 10^{17} cm^{-3}) also eliminate possible effects due to saturation of occupied traps. Furthermore, the use of optically thin films of silicon minimize diffusion of the free carriers from the probing region, since carriers are injected throughout the silicon in the optically pumped region. These conditions assure that the measured carrier lifetimes are primarily determined by the free-carrier trapping and recombination.

The samples used in this study consist of $0.5\text{ }\mu\text{m}$ silicon-on-sapphire wafers that were implanted at room temperature with O^+ ions at 200 and 100 keV energies. These ion energies were chosen to provide a $0.5\text{-}\mu\text{m}$ implant depth with damage dispersed throughout the entire silicon film. The samples with doses ranging from $1 \times 10^{12}\text{ cm}^{-2}$ to $1 \times 10^{14}\text{ cm}^{-2}$ were implanted with 200 keV ions while the more highly implanted samples (up to $7.5 \times 10^{15}\text{ cm}^{-2}$) received approximately equal doses at both energies.

Time-resolved reflectivity and transmission measurements were obtained following excitation with femtosecond optical pulses. The laser source is a compensated colliding-pulse, mode-locked dye laser producing 70 fs pulses at 625 nm (2.0 eV) at a repetition rate of 100 MHz. These pulses are split into two beams to provide the pump and probe pulses. The average power of the pump beam was in the range 0.1–2.0 mW (1–20 pJ/pulse) and is focused to a diameter of about $10\text{ }\mu\text{m}$. The probe beam, attenuated to 1–5% of the pump power, is focused to a diameter of about $5\text{ }\mu\text{m}$. The polarization of the probe beam is rotated by 90° to suppress interferences between the two beams on the sample surface. The pump is incident on the sample at an angle of 30° relative to the normal while the probe is incident on the opposite side of the normal at an angle of 60° . The pump beam is chopped at 1 kHz. Before reaching the sample, the probe beam is additionally split into two beams: one is reflected off the sample onto a photodiode detector and the other, incident directly onto a matched photodiode, is used as a reference. The reflection signal is derived as the difference of these two photocurrents and is detected, using a lock-in amplifier, as a function of time delay between the pump and probe pulses. The sensitivity of our apparatus to changes in the probe beam reflectance is approximately 1 part in 10^6 .

Without pumping, the reflectivity at normal incidence of the samples used in this study at 625 nm is relatively constant at a value of 0.2 and increases only slightly at the highest implantation dose. The reflectivity of unimplanted SOS and amorphous silicon is also very similar with values of 0.2 and 0.25. The absorption, however, increases monotonically from 0.3 at a dose $1 \times 10^{12}\text{ cm}^{-2}$ to 0.65 at the highest dose of $7.5 \times 10^{15}\text{ cm}^{-2}$. For the unimplanted SOS and amorphous silicon ($0.3\text{ }\mu\text{m}$ thickness) the measured absorptions are 0.25 and 0.6, respectively.

The time evolution of the change in reflectivity following photoexcitation of two representative samples is shown in Fig. 1. Figure 1(a) was obtained for an SOS sample ion

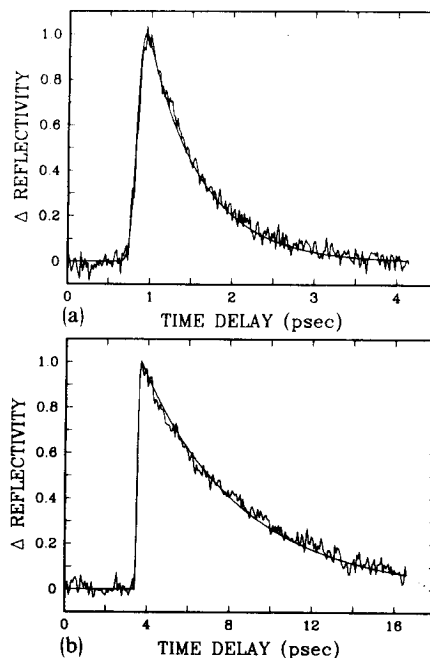


FIG. 1. Measured change in reflectivity for SOS samples ion implanted at doses of (a) $2 \times 10^{15}\text{ cm}^{-2}$ and (b) $1 \times 10^{13}\text{ cm}^{-2}$. Smooth curves are fits obtained using a 140 fs instrument response convoluted with (a) 0.65 ps and (b) 4.8 ps exponential decays.

implanted at a dose of $2 \times 10^{15}\text{ cm}^{-2}$, while Fig. 1(b) was obtained at a dose of $1 \times 10^{13}\text{ cm}^{-2}$. The data exhibit a fast rise ($< 150\text{ fs}$) followed by a slower recovery back toward normal reflectivity. The peak change in reflectivity ($\Delta R/R$) of the data in Fig. 1 is approximately 10^{-5} . This value is in agreement with the expected index change predicted by Eq. (3) for our experimental conditions ($\Delta n/n_0 \sim 10^{-5}$).

The time evolution of the change in reflectivity is consistent with a pulse width limited rise and an exponential recovery. To obtain fits to the data, we approximated our pump/probe experimental response function as a 140 fs Gaussian. The smooth curves also shown in Fig. 1 were obtained by a convolution of the instrument response with exponential decays of 650 fs [Fig. 1(a)] and 4.8 ps [Fig. 1(b)]. At the signal-to-noise levels of these results, a simple exponential recovery accurately describes the time evolution of the change in reflectivity.

Femtosecond resolved reflectivity data were obtained for a series of SOS samples with a range of implantation doses covering four orders of magnitude and also for amorphous silicon and unimplanted SOS. In attempting to interpret these data, each curve was fit to a single exponential decay time, which varied from $> 300\text{ ps}$ for the unimplanted SOS wafer down to about 600 fs for the amorphous and the highly implanted samples. These results are summarized in Fig. 2. There are two major regions of interest: the variation of the lifetime at low ion-implantation doses, $< 1 \times 10^{14}\text{ cm}^{-2}$, and the lack of dependence at the higher doses, $> 3 \times 10^{14}\text{ cm}^{-2}$.

At low implant levels, the lifetime decreases linearly with increasing ion-implantation dose. This is clearly demonstrated by the fit of the low dose data points in Fig. 2 to a

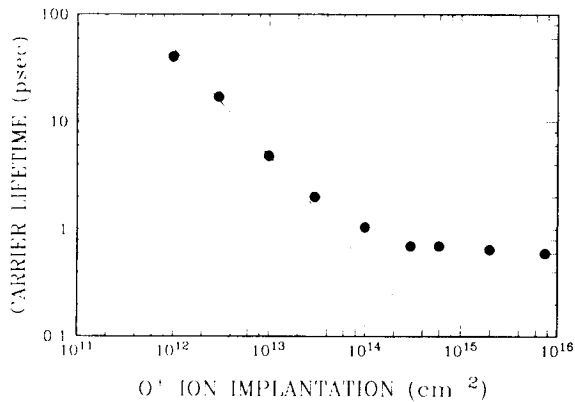


FIG. 2. Carrier lifetime vs ion-implantation dose. Lifetimes are derived from individual reflectivity data at each dose. The solid line shown has a slope of unity.

slope of unity. The linear dependence in this region is consistent with recombination rates proportional to the density of traps introduced by the ion implantation. This behavior is predicted by an expression, valid for low carrier densities, that estimates the capture time τ by traps in crystals as¹³

$$1/\tau = N_t \sigma \langle v \rangle, \quad (4)$$

where N_t is the trap density, σ is the capture cross section, and $\langle v \rangle$ is the average carrier thermal velocity. In this case, the trap density and therefore the free-carrier trapping rate will vary linearly with ion-implantation level.

The variation of lifetime with implantation dosage saturates at a level $3 \times 10^{14} \text{ cm}^{-2}$. Above this dose, the lifetime reaches a limit of 600 fs. This lifetime does not vary even as the implantation dose is increased by more than a factor of 20. Shorter lifetimes are clearly resolvable by our experimental resolution as evidenced by the < 150 fs rise times of the data presented in Fig. 1. The approximate 600-fs limit is therefore due to the response of the semiconductor itself. This behavior is not expected from Eq. (4) which predicts a continuous decrease in lifetime with implantation dose.

One possible explanation for the lack of the carrier lifetime dependence on ion-implantation dose is hot-carrier relaxation. The photoexcitation energy of 2.0 eV is significantly larger than the band gap (1.15 eV for pure Si). The 600-fs lifetime limit may therefore represent the thermalization time of the photoexcited carriers as they relax toward the band edge. This process will act as a bottleneck to trapping of the carriers. However, one would not necessarily expect the same relaxation rate for Si at all implant doses, or that only thermalized carriers are trapped. Furthermore, no experimental evidence such as nonexponential behavior in the reflectivity measurements, was observed.

The most probable process limiting the carrier lifetime

is amorphization of the crystalline silicon. Above a critical dose of $3 \times 10^{14} \text{ cm}^{-2}$ the density of effective traps introduced by implantation saturates and the sample is essentially amorphous. The reflectivity data obtained for amorphous silicon also exhibit the same carrier lifetime of 600 fs. This interpretation is supported by electron spin resonance¹⁴ and third harmonic generation¹⁵ studies on ion-implanted SOS which showed similar saturation effects occurring at critical implantation doses of 10^{14} – 10^{15} cm^{-2} .

In summary, we have measured the dependence of the free-carrier lifetime on ion-implantation dose in silicon. At low implant doses, the carrier trapping rate ($1/\tau$) increased linearly with the trap density introduced by radiation damage. At doses above a critical dose of $3 \times 10^{14} \text{ cm}^{-2}$ the measured carrier lifetime reaches a limit of 600 fs. This limit is believed to be due to amorphization or a saturation of the effective trap density in the crystalline silicon. For high-speed optoelectronics, the carrier lifetime saturation effect implies that the 0.6-ps electrical pulses produced by Ketchen *et al.*⁴ is the limiting pulse width that can be produced using devices fabricated on ion-implanted SOS.

We would like to acknowledge the many stimulating and informative discussions with I. N. Duling, III and J. A. Kash. This research was partially supported by the U. S. Office of Naval Research.

¹D. H. Auston, in *Picosecond Optoelectronic Devices*, edited by C. H. Lee (Academic, London, 1984), pp. 73–116.

²J. A. Valdmanis, G. A. Mourou, and C. W. Gabel, *IEEE J. Quantum Electron.* **QE-19**, 664 (1983).

³G. A. Mourou, and K. E. Meyer, *Chem. Phys. Lett.* **45**, 492 (1984).

⁴M. B. Ketchen, D. Grischkowsky, T. C. Chen, C.-C. Chi, I. N. Duling, III, N. J. Halas, J.-M. Halbout, J. A. Kash, and G. P. Li, *Appl. Phys. Lett.* **48**, 751 (1986).

⁵See, for example, *Picosecond Electronics and Optoelectronics*, edited by G. A. Mourou, D. H. Bloom, and C.-H. Lee (Springer, New York, 1985).

⁶P. R. Smith, D. H. Auston, A. M. Johnson, and W. M. Augustyniak, *Appl. Phys. Lett.* **38**, 47 (1981).

⁷D. H. Auston, K. P. Cheung, and P. R. Smith, *Appl. Phys. Lett.* **45**, 284 (1984).

⁸D. von der Linde and N. Fabricius, *Appl. Phys. Lett.* **41**, 991 (1982).

⁹L. A. Lompre, J. M. Liu, H. Kurz, and N. Bloembergen, in *Ultrafast Phenomena IV*, edited by D. H. Auston and K. B. Eisenthal (Springer, New York, 1984), p. 122.

¹⁰C. V. Shank, R. Yen, and C. Hirlimann, *Phys. Rev. Lett.* **50**, 454 (1983).

¹¹L.-A. Lompre, J.-M. Liu, H. Kurz, and N. Bloembergen, *Appl. Phys. Lett.* **44**, 3 (1984).

¹²M. C. Downer and C. V. Shank, *Phys. Rev. Lett.* **56**, 761 (1986).

¹³C. T. Sah, R. N. Noyce, and W. Shockley, *Proc. IRE* **45**, 1228 (1957).

¹⁴J. R. Dennis and E. B. Hale, *J. Appl. Phys.* **49**, 1119 (1978).

¹⁵C. C. Wang, J. Bomback, W. T. Donlon, C. R. Huo, and J. V. James, *Phys. Rev. Lett.* **57**, 1647 (1986).